

# Reduction of Glucose Uptake through Inhibition of Hexose Transporters and Enhancement of Their Endocytosis by Methylglyoxal in *Saccharomyces cerevisiae*\*

Aya Yoshida, Dandan Wei, Wataru Nomura, Shingo Izawa<sup>1</sup>, and Yoshiharu Inoue

Laboratory of Molecular Microbiology, Division of Applied Life Sciences, Graduate School of Agriculture, Kyoto University, Uji, Kyoto 611-0011, Japan

\*Running title: Methylglyoxal inhibits glucose uptake

<sup>1</sup> Present address: Laboratory of Microbial Technology, Graduate School of Science and Technology, Kyoto Institute of Technology, Kyoto, Japan

Address correspondence to Yoshiharu Inoue, Laboratory of Molecular Microbiology, Division of Applied Life Sciences, Graduate School of Agriculture, Kyoto University, Uji, Kyoto 611-0011, Japan. Tel.: +81 774-38-3773, Fax: +81 774-38-3789; E-mail: y\_inoue@kais.kyoto-u.ac.jp

**Keywords:** hexose transporter, *Saccharomyces cerevisiae*, methylglyoxal, endocytosis, Rsp5, phospholipase C

---

**Background:** Methylglyoxal is a typical 2-oxoaldehyde derived from glycolysis.

**Results:** Methylglyoxal inhibited the activity of yeast hexose transporters as well as mammalian glucose transporters (GLUT1 and GLUT4), and enhanced the endocytosis of hexose transporters in yeast.

**Conclusion:** Methylglyoxal inhibited glucose uptake in yeast cells.

**Significance:** Phospholipase C and protein kinase C were involved in endocytosis of hexose transporters.

Diabetes mellitus is characterized by an impairment of glucose uptake even though blood glucose levels are increased. Methylglyoxal is derived from glycolysis, and has been implicated in the development of diabetes mellitus, because methylglyoxal levels in blood and tissues are higher in diabetic patients than in healthy individuals. However, it remains to be elucidated whether such factors are a cause, or consequence, of diabetes. Here we show that methylglyoxal inhibits the activity of mammalian glucose transporters using recombinant *Saccharomyces cerevisiae* cells genetically lacking all hexose transporters but carrying cDNA for human GLUT1 or rat GLUT4. We found that methylglyoxal

inhibits yeast hexose transporters also. Glucose uptake was reduced in a stepwise manner following treatment with methylglyoxal, *i. e.* a rapid reduction within 5 min, followed by a slow and gradual reduction. The rapid reduction was due to the inhibitory effect of methylglyoxal on hexose transporters, while the slow and gradual reduction seemed due to endocytosis, which leads to a decrease in the amount of hexose transporters on the plasma membrane. We found that Rsp5, a HECT-type ubiquitin ligase, is responsible for the ubiquitination of hexose transporters. Intriguingly, Plc1 (phospholipase C) negatively regulated the endocytosis of hexose transporters in an Rsp5-dependent manner, although the methylglyoxal-induced endocytosis of hexose transporters occurred irrespective of Plc1. Meanwhile, the internalization of hexose transporters following treatment with methylglyoxal was delayed in a mutant defective in protein kinase C.

---

Glucose is an easy-to-use energy source for all kinds of cells. However, since cellular membranes are not very permeable to glucose, cells are equipped with glucose transporters on the plasma membrane to take

up glucose from outside of the cell. Many glucose transporters from prokaryotes to higher eukaryotes belong to the major facilitator superfamily (MFS), which is characterized by a single-polypeptide carrier with twelve transmembrane domains capable of transporting substrates across the membrane in response to a chemiosmotic gradient (1-3). For example, if the glucose concentration outside of cells is higher, glucose transporters take up glucose from outside, but when the intracellular glucose concentration is higher than outside, they pump out glucose.

Although glucose is necessary as an energy source, glucose homeostasis in blood is crucial for mammals. Diabetes mellitus is characterized by a disruption of glucose homeostasis. When blood glucose levels increase upon food-intake, insulin is secreted from pancreatic  $\beta$  cells. The insulin signaling pathway in cells possessing insulin receptors is activated upon receipt of insulin, which leads to the translocation of a glucose transporter, GLUT4, to the plasma membrane thereby facilitating the influx of glucose (4). In type 1 diabetes, insulin secretion is defective; whereas in type 2 diabetes, cells are insensitive to insulin (insulin resistance), which seems to be caused by lifestyle. In both cases, cells are impaired in taking up glucose from blood, and consequently, hyperglycemic situations develop, which leads to the induction of several diabetic complications. One of the causes of diabetic complications is the accumulation of advanced glycation end products (AGEs), the synthesis of which is initiated by a non-enzymatic reaction between the aldehyde groups of glucose and amino groups of proteins, sometimes referred to as the Maillard reaction (5). Methylglyoxal (MG,  $\text{CH}_3\text{COCHO}$ ) is a ubiquitous 2-oxoaldehyde derived from glycolysis (6-8). Because MG contains two carbonyl groups, it has a 20000-fold higher potential than glucose to produce AGEs (9). Therefore, MG levels and diabetic complications are closely related (10). The levels of MG in blood and tissues are higher in diabetic patients than healthy individuals (11-13). However, it remains to be solved whether high MG levels are a cause, or a consequence, of diabetes. Furthermore, the correlation between the onset of hyperglycemic conditions and an increase in MG levels has not been well investigated.

One feature of diabetes mellitus is that the hyperglycemia is sustained even in a fasted

state. The control of blood glucose levels mainly depends upon whether glucose transporters can transport glucose adequately (14, 15). To date, thirteen glucose transporters, GLUT1-GLUT12 and Hmit1, have been identified in mammals (2, 3). These transporters are responsible for the supply of glucose to various tissues, storage of glucose (glycogen) in liver, uptake of glucose in response to insulin, and sensing of blood glucose levels in pancreatic  $\beta$  cells (16-18). Mammalian glucose transporters are classified into three groups on the basis of primary structure (19). GLUT1-GLUT4 belong to MFS (3). GLUT1, the first glucose transporter to be identified (20), is distributed in almost all tissues, and therefore, is thought to play a crucial role in glucose homeostasis under normal conditions (19). Since only GLUT4 is sensitive to insulin, it is involved in controlling blood glucose levels upon food-intake (15).

Since yeast has served as a model of higher eukaryotes to reveal the mechanisms of many pivotal biological events, it is feasible that we will gain a clue as to the effect of MG on the function of mammalian GLUTs by analyzing the effect of MG on yeast glucose transporters. In the budding yeast *Saccharomyces cerevisiae*, glucose transporters are referred to as hexose transporters (Hxts). *S. cerevisiae* has seventeen hexose transporters (Hxt1-Hxt17), and Gal2 as a galactose permease, all of which belong to MFS (21). We found that MG inhibits the activities of not only yeast Hxts but also mammalian GLUTs. Furthermore, MG induced endocytosis of yeast Hxts in an Rsp5 (HECT-type ubiquitin ligase)-dependent manner, thereby lowering glucose uptake. We found that protein kinase C (Pkc1) is involved in the MG-induced endocytosis of Hxts. Intriguingly, a deficiency in phospholipase C (Plc1) accelerated the internalization of Hxts under normal conditions in an Rsp5-dependent manner. However, the MG-induced endocytosis of Hxts occurred independently of Plc1.

## MATERIALS AND METHODS

### *Media*

The media used were YPD (2% glucose, 1% yeast extract, 2% peptone), YPMal (2% maltose, 1% yeast extract, 2% peptone), SD (2% glucose, 0.67% yeast nitrogen base w/o amino acids), SGal (2% galactose, 0.67% yeast nitrogen base w/o amino acids), and SMal (2% maltose, 0.67% yeast

nitrogen base w/o amino acids). Appropriate amino acids and bases were added to the SD, SGal, and SMal media as necessary. To select the *HXT* null mutant carrying a plasmid (*URA3* marker) harboring human GLUT1 cDNA or rat GLUT4 cDNA, cells were first spread on to YPMal agar (2%) plates after transformation, and cells grown on YPMal agar plates were replica plated on SMal agar plates without uracil. After verification of growth in SMal agar plates without uracil, cells were streaked on SD agar plates without uracil to verify the functional expression of GLUT1 and GLUT4.

#### Strains

Yeast strains used are summarized in Table 1. To construct an *rsp5<sup>wimp</sup>* (*RSP5* low-level-expression) mutant with the YPH250 background, the *natMX*-inserted *RSP5* promoter region of EN44 (22) was amplified by PCR with primers RSP5-F and RSP5-R-2. The PCR fragment was introduced into the *RSP5* locus of YPH250. To construct a *plc1Δ* mutant, a *plc1Δ::HIS3* allele of YJF32 (23) was amplified by PCR with PLC1-F and PLC1-R-2, and the product was introduced into the wild-type strain or *rsp5<sup>wimp</sup>* mutant of YPH250. To disrupt the *SCH9* gene in YPH250, a *sch9Δ::TRP1* allele of TVH301 (24) was amplified with primers SCH9-F and SCH9-R, and the amplicon was introduced into YPH250. Primers used in this study are summarized in Supplemental Table S1.

#### Plasmids

To construct the integration plasmids for Hxt1-GFP, Hxt2-GFP, and Hxt3-GFP, each *HXT* gene (*HXT1*, +401 ~ +1720; *HXT2*, +304 ~ +1640; and *HXT3*, +687 ~ +1724) was amplified with the following primer sets: *HXT1*, HXT1-F-XbaI plus HXT1-R-XhoI; *HXT2*, HXT2-F-XbaI plus HXT2-R-XhoI; and *HXT3*, HXT3-F-XbaI plus HXT3-R-XhoI. Each PCR product was digested with XbaI and XhoI, and the resultant fragment was introduced into the XhoI and XbaI sites of YIp-*NUP116*-GFP (25), a pRS306 backbone plasmid, to replace *NUP116* with each *HXT* gene. The plasmids constructed (pHXT1-GFP, pHXT2-GFP, and pHXT3-GFP) were digested with HpaI, and the linearized DNA was introduced at the loci of *HXT1*, *HXT2*, and *HXT3*, respectively, to replace each gene containing a GFP tag.

We verified that each Hxt-GFP protein is functional as glucose transporter by evaluating the recovery of growth of K73 cells in glucose medium. Because K73 lacks *HXT1-7*, it is not able to grow in glucose medium (26). However, since *HXT1*, *HXT2*, and *HXT3* are deleted in K73, we cannot integrate GFP into each *HXT* locus to construct *HXT-GFPs*. So, we constructed plasmid-borne Hxt-GFPs. YIp-*NUP116*-GFP (25) was digested with XhoI and KpnI, and the XhoI-KpnI fragment containing GFP and *NUP2* 3' UTR was cloned into the XhoI-KpnI sites of pRS316. The resultant plasmid was named

pRS316-GFP. Each *HXT* gene with its own promoter was amplified by PCR with the following primer sets: *HXT1*, HXT1-F-SacI plus HXT1-R-XhoI; *HXT2*, HXT2-F-SacI plus HXT2-R-XhoI; and *HXT3*, HXT3-F-SacI plus HXT3-R-XhoI. Each PCR product was digested with SacI and XhoI, and the resultant fragment was cloned into the SacI and XhoI sites of pRS316-GFP. The plasmids constructed (pRS316+HXT1-GFP, pRS316+HXT2-GFP, pRS316+HXT3-GFP) contain the same *HXT-GFP* allele with that of the genome-integrated *HXT-GFP* gene. K73 cells carrying each plasmid were able to grow in glucose medium, indicating that Hxt1-GFP, Hxt2-GFP, and Hxt3-GFP proteins are functional as glucose transporters.

To construct the integration plasmids for *HXT1-lacZ*, *HXT2-lacZ*, and *HXT3-lacZ*, the promoter region of each *HXT* gene was amplified with the following primer sets: *HXT1*, HXT1-lacZ-F plus HXT1-lacZ-R; *HXT2*, HXT2-lacZ-F plus HXT2-lacZ-R; and *HXT3*, HXT3-lacZ-F plus HXT3-lacZ-R. Each PCR product was digested with Sall and EcoRI, and the resultant fragment was introduced into the Sall and EcoRI sites of YIp358R. The plasmids constructed (YIp358R+HXT1-lacZ, YIp358R+HXT2-lacZ, and YIp358R+HXT3-lacZ) were digested with NcoI, and integrated into the *ura3-52* locus of the wild-type and *plc1Δ* mutant of YPH250.

Plasmids used in this study are summarized in Table 2.

#### Glucose uptake experiment

Cells were cultured in SD medium until a log phase of growth, and 10 mM MG was added. Next, 5 ml of culture was taken at the prescribed time and transferred to a 15-ml falcon tube, and 10  $\mu$ l of [<sup>14</sup>C]-glucose (10.6 GBq/mmol, GE Healthcare Bio-Science) was added. Cells were then collected, washed with a chilled 0.85% NaCl solution, and suspended in 200  $\mu$ l of distilled water. The cell suspension (150  $\mu$ l) was mixed with 2 ml of a liquid scintillation cocktail (Ulutima-Flo AP, Perkin Elmer), and the amount of [<sup>14</sup>C]-glucose taken up by cells was measured using a scintillation counter (LS6500, BECKMAN COULTER). When cells were treated with latrunculin B (Lat-B, BIOMOL International), cells were pretreated with 100  $\mu$ M Lat-B for 20 min prior to the addition of MG.

#### Western blotting of GFP-tagged Hxts

Cells carrying Hxt1-GFP, Hxt2-GFP, or Hxt3-GFP were cultured in 200-ml flasks containing 50 ml of SD medium until a log phase of growth ( $A_{610} \approx 0.5$ ), 10 mM MG was added, and the cells were incubated for the prescribed time. After being collected by centrifugation, cells were disrupted with glass beads in 100  $\mu$ l of buffer A [50 mM Tris-HCl (pH 8.0), 10 mM EDTA, 5% glycerol, and protease inhibitor cocktail (Nacalai tesque)] using BeadSmash 12

(Waken). Cell homogenates were kept on ice for 2 min, and transferred to another tube. The resulting glass beads were mixed with 100  $\mu$ l of buffer A, and kept on ice for 2 min. The supernatant was mixed with the first cell homogenate, which was then centrifuged at low speed (3000 rpm for 2 min at 4°C) to remove unbroken cells and cell debris, and the resultant supernatant, referred to as whole cell extract (WCE), was transferred to another tube. WCE was centrifuged at 14000 rpm for 15 min at 4°C, and the supernatant (soluble fraction) and pellet (insoluble fraction) were separated. The pellet was suspended in 75  $\mu$ l of IPP150 buffer [10 mM Tris-HCl (pH 8.0), 150 mM NaCl, and 0.1% NP40] containing 1% *n*-octyl- $\beta$ -D-glucoside (Dojin) and protease inhibitor cocktail, and the suspension was kept on ice for 1 h, then centrifuged at 14000 rpm for 10 min at 4°C. The supernatant was used as a membrane fraction. The soluble fraction (4  $\mu$ g of protein) and membrane fraction (40  $\mu$ g of protein) were subjected to SDS-PAGE. Separated proteins were transferred onto a PVDF membrane (Millipore) then detected using anti-GFP monoclonal antibody (Santa Cruz). Immunoreacted bands were visualized with a kit (Immobilon Western chemiluminescent HRP Substrate, Millipore) using a LAS-4000mini imaging system (FUJIFILM).

#### Detection of ubiquitination

To prepare the membrane fraction containing protein A-tagged Hxt2 (Hxt2-PA), MBY242 cells carrying the *HXT2-PA* gene (27) were cultured in SD medium until a log phase of growth, then transferred to fresh medium containing 0.1% glucose and 0.67% yeast nitrogen base (w/o amino acids) supplemented with appropriate amino acids and bases. After 1 h, cells were collected and disrupted as described above. WCE was ultracentrifuged at 50000 rpm for 1 h at 4°C (himac CS120, Hitachi). The pellet was suspended in buffer A, and ultracentrifuged again. The resultant pellet was suspended in IPP150 buffer containing 1% *n*-octyl- $\beta$ -D-glucoside. After a 1-h incubation on ice, the cell suspension was centrifuged at 14000 rpm for 10 min at 4°C, and the supernatant was transferred to a tube containing 50  $\mu$ l of IgG beads (IgG Sepharose™ 6 Fast Flow, Amersham Biosciences) equilibrated with IPP150 buffer. To adsorb the protein A-tagged Hxt2 to IgG beads, the mixture was gently rotated at 4°C for 2 h. Subsequently, IgG beads were washed with 1 ml of IPP150 buffer three times, and then 0.9 ml of 100 mM glycine-HCl buffer (pH 3.5) was added to elute Hxt2-PA. After centrifugation, the supernatant was mixed with 100% trichloroacetic acid (final concentration, 10%), and the mixture was kept on ice for 10 min to precipitate proteins. After removal of the supernatant by centrifugation (14000 rpm, 10 min, 4°C), the pellet was washed with acetone, and dried materials were dissolved in 25  $\mu$ l of 1 M Tris-HCl (pH 7.5). After which, 25  $\mu$ l of 2x SDS-PAGE sample buffer was added, and the mixture was boiled for 3 min. Protein

concentrations were determined using a RC DC Protein Assay kit (Bio-Rad). After SDS-PAGE followed by the transfer of separated proteins onto a PVDF membrane, Hxt2-PA and its ubiquitinated form were detected using anti-protein A (LOCKLAND) and anti-ubiquitin (BIOMOL International LP) antibodies, respectively.

#### Western blotting of Hxts1/2 and GLUTs1/4

KY73 (*hxt1-7 $\Delta$* ) (26) carrying a plasmid harboring *HXT1* or *HXT2*, EBY.S7 (*hxt $\Delta$  fgy1-1*) (28) carrying GLUT1 cDNA, or EBY.F4-1 (*hxt $\Delta$  fgy1-1 fgy4-1*) (28) carrying GLUT4 cDNA was cultured in SD medium until a log phase of growth, and the membrane fraction was prepared by ultracentrifugation as described above. Anti-Hxt1, anti-Hxt2, anti-GLUT1, and anti-GLUT4 antibodies, which were donated by Dr. T. Kasahara, were used to detect proteins. To detect Pma1, an anti-Pma1 antibody (Encor Biotechnology) was used.

#### Microscopy

Cells carrying GFP-tagged proteins were cultured in SD medium until a log phase of growth, and 10 mM MG was added. The localization of each protein of interest was determined periodically using a fluorescence microscope. To stain vacuoles, 10 ml of culture was centrifuged to collect cells, which were then suspended in 196  $\mu$ l of YPD medium. Four microliters of 2 mM FM4-64 (Biotium) was added to the cell suspension, and incubated at 28°C in the dark. After 20 min of incubation, 1 ml of a 0.85% NaCl solution was added to the cell suspension, and centrifuged to collect the cell. Cells were then suspended in fresh SD medium, and incubated for the prescribed time in the presence or absence of MG at 28°C.

## RESULTS

#### MG inhibits glucose uptake in yeast

To explore the effect of MG on the function of hexose transporter (Hxt), we determined the rate of glucose uptake by yeast cells in the presence of MG. [<sup>14</sup>C]-Glucose was added to the culture in which yeast cells were growing logarithmically, and the amount of [<sup>14</sup>C]-glucose taken up by cells was determined. Figure 1A shows the levels of [<sup>14</sup>C]-glucose uptake after 15 min of addition of various concentrations of MG. Glucose uptake was inhibited in the presence of MG in a dose-dependent manner, and approximately 50% inhibition was attained by 10 mM MG. Next, we determined the time course of the effect of MG on inhibition of glucose uptake. The rate of uptake dropped by 35% within the first 5 min after

the addition of 10 mM MG, after which it declined gradually. It had decreased by approximately 60% after 60 min compared with that in the absence of MG. Several explanations are feasible regarding the reduction of glucose uptake following treatment with MG. For example, MG inhibited the activity of Hxts, or the number of Hxt molecules on the plasma membrane was decreased by endocytosis followed by degradation in vacuoles. To study these possibilities, we first determined whether endocytosis of Hxts occurred upon MG stress.

#### *MG induces the degradation of Hxts*

*S. cerevisiae* has seventeen *HXT* genes encoding glucose transporters. Since a mutant lacking one of these *HXT* genes is able to grow in a medium containing glucose as a source of carbon, these Hxts share redundant functions in terms of glucose uptake (21). However, since a mutant lacking *HXT1* to *HXT7* simultaneously loses the ability to grow in glucose medium (26), the rest of Hxts does not seem to play crucial roles in glucose uptake. The mRNAs of *HXT1*, *HXT2*, and *HXT3* were abundant compared with those of other *HXTs* in cells cultured under ordinary laboratory conditions (*i. e.* containing 2% glucose) (29), so we determined the localization of GFP-tagged Hxt1, Hxt2, and Hxt3 as representatives of Hxts using a fluorescence microscope.

As shown in Fig. 2A, Hxt1-GFP, Hxt2-GFP, and Hxt3-GFP were located on the plasma membrane at a log phase of growth, however, small punctate vesicles appeared after 15 min of MG treatment, which grew in size (30~60 min), and fluorescence derived from GFP-tagged proteins was observed in vacuoles (60~120 min). We investigated whether membrane proteins in general are also internalized following treatment with MG; however, other proteins such as Pmal (plasma membrane H<sup>+</sup>-ATPase) and Rvs161 (Amphiphysin-like lipid raft protein) were not internalized upon MG treatment (Fig. 2B).

To verify whether the amount of Hxt1~3 on the plasma membrane is decreased following treatment with MG, Western blotting was conducted. As shown in Fig. 2C, the levels of Hxt1-GFP, Hxt2-GFP, and Hxt3-GFP in membrane fractions decreased with time. By contrast, the levels of GFP protein in soluble fractions, which are derived from GFP-tagged Hxt1~3 by degradation in vacuoles, were increased.

These results indicate that Hxt1~3 are internalized and degraded in the vacuole following treatment with MG.

#### *MG induces endocytosis of Hxts*

The endocytotic membrane vesicles fuse with endosomes, on which membrane the ubiquitin-modified cargo proteins are located, and subsequently, the components constituting the ESCRT (endosomal sorting complex required for transport) assemble on the endosomal membrane to internalize the cargo proteins into the lumen of endosomes, which are referred to as multivesicular bodies (MVBs) (30). The deubiquitination is preceded by the internalization of cargo proteins into the luminal side of endosomes. In yeast cells, Doa4 is responsible for the deubiquitination of ubiquitin-modified cargo proteins in this process (31). The MVBs containing the internalized vesicles with deubiquitinated cargo proteins fuse with vacuoles, and consequently, degradation of MVBs occurs in the lumen of vacuoles. If deubiquitination of ubiquitin-modified cargo proteins does not occur, such endosomes are not able to develop to MVBs, and therefore, unable to fuse with vacuoles (31). Such endosomes form the so-called “ring-like structure” in the immediate vicinity of the vacuole, which can be visualized by staining endosomal membranes with a fluorescent dye, FM4-64 (32). To verify whether internalized Hxts are transported into the vacuole, we stained cells for vacuoles with FM4-64, and localization of Hxt1/2/3-GFPs was determined following treatment with MG. As shown in Fig. 3, GFP signals of each Hxt-GFP were observed in the vacuole, which was visualized with FM4-64. Next, to investigate whether transportation of Hxt1~3 into the vacuole in the presence of MG is performed *via* the MVB pathway, we monitored the localization of Hxt1/2/3-GFPs in *doa4Δ* cells. As shown in Fig. 3, GFP-tagged Hxt1~3 accumulated in close proximity to the vacuolar membrane to form the ring-like structure, and no fluorescence signal was detected from the vacuolar lumen in *doa4Δ* cells. These results indicate that endocytosis of Hxts occurs upon MG treatment, and subsequently, internalized Hxts are transported into vacuoles *via* the MVB pathway for degradation.

#### *MG inhibits the activity of Hxt*

We have demonstrated that MG induces the internalization of Hxt1, Hxt2, and Hxt3, thereby seemingly reducing the ability of

yeast cell to take up glucose. The reduction of glucose uptake following treatment with MG occurred in a stepwise manner, *i. e.* a rapid response within 5 min, and a slow and gradual response thereafter (Fig. 1B). Since the internalization of Hxts occurred relatively slowly, the reduction in glucose uptake that occurred within 5 min is not likely dependent upon a decrease in the number of Hxts on the plasma membrane. To determine whether a rapid reduction of glucose uptake upon MG stress occurs irrespective of the endocytosis of Hxts, we measured glucose uptake under conditions where endocytosis is blocked. The actin cytoskeleton plays a crucial role in endocytosis, therefore, the depolymerization of F actin blocks endocytosis. Latrunculin B (Lat-B) as well as Lat-A depolymerizes F actin (33), thereby blocking endocytosis (34). We verified that endocytosis of Hxt1/2/3-GFPs following treatment with MG was blocked when Lat-B was present (Fig. 4A). Then, we determined glucose uptake within the first 5 min of treatment with MG in the presence of Lat-B. As shown in Fig. 4B, the reduction in glucose uptake was substantially the same as that without Lat-B, suggesting that MG inhibits the activity of Hxt *per se*, and a rapid reduction in glucose uptake occurs irrespective of the endocytosis of Hxts.

#### *MG inhibits Hxt1 and Hxt2*

Next, to explore whether the inhibitory effect of MG on glucose uptake differs depending upon the Hxt's affinity for glucose, we used a mutant (K73) lacking *HXT1-HXT7* (*hxt1-7Δ*) but carrying a plasmid harboring either *HXT1* or *HXT2*. K73 cells are not able to grow in glucose medium but in maltose medium, because the maltose permeases in K73 remain intact (26). *HXT1* codes for a low-affinity glucose transporter, and *HXT2*, a high-affinity transporter (21). We verified that the growth of K73 cells in glucose medium was restored by the introduction of a plasmid harboring either *HXT1* or *HXT2*, which indicates that the introduced *HXT1* and *HXT2* are functionally active in K73 cells. We verified by Western blotting that the Hxt1 and Hxt2 proteins were adequately located on the plasma membrane (Fig. 5A). We determined the glucose uptake using the resultant transformants. As shown in Fig. 5B, the glucose uptake was inhibited in K73 cells expressing *HXT1* or *HXT2* following treatment with MG, suggesting that the inhibitory effect of MG on the activity of Hxt is exerted irrespective of its affinity for

glucose.

#### *MG inhibits mammalian GLUTs*

Since we revealed that MG inhibits the activity of a yeast glucose transporter or Hxt, next we determined whether MG inhibits the activity of a mammalian glucose transporter (GLUT) also. To explore the effect of MG on the activity of GLUT using a yeast system, we used EB.Y.S7 carrying a human GLUT1 cDNA, and EB.Y.F4-1 carrying a rat GLUT4 cDNA. Both EB.Y.S7 and EB.Y.F4-1 lack all *HXT* genes (28). We verified the expression of human GLUT1 and rat GLUT4 by Western blotting using anti-GLUT1 and anti-GLUT4 antibodies, respectively (Fig. 6A). In addition, the validity of the function of GLUT1 and GLUT4 expressed in yeast cells was verified by the ability of each transformant to grow in glucose medium, because these *hxt* null mutants (EB.Y.S7 and EB.Y.F4-1) are not able to grow in medium containing glucose as a sole source of carbon (28). As shown in Fig. 6B, glucose uptake in cells carrying human GLUT1 or rat GLUT4 was lowered following treatment with MG in the presence of Lat-B. These results indicate that MG inhibits mammalian glucose transporters.

#### *MG-induced endocytosis of Hxts is dependent upon Rsp5*

The results obtained led us to conclude that the rapid reduction in glucose uptake following treatment with MG is due to its inhibitory effect on Hxts. So, next, we explored the mechanism behind the MG-induced endocytosis of Hxts.

Generally, ubiquitination, in many cases mono-ubiquitination, is a trigger for the endocytosis of membrane-integral proteins on the plasma membrane (35). So, we determined whether ubiquitination of Hxt occurs following treatment with MG. In the ubiquitination of many transporters and permeases on the plasma membrane in *S. cerevisiae*, Rsp5, a HECT-type ubiquitin ligase, plays an important role (36). To explore whether MG-induced endocytosis of Hxt1~3 is dependent upon Rsp5, we constructed an *rsp5<sup>wimp</sup>* mutant. Because the *RSP5* gene is essential, an *rsp5* null mutant is unavailable. So, we inserted the *natMX* gene into the promoter of *RSP5* to decrease its expression level (22). As shown in Fig. 7A, the MG-induced endocytosis of Hxts was inhibited in *rsp5<sup>wimp</sup>* cells. We verified that the amounts of Hxt1, Hxt2, and Hxt3 in membrane fractions did not decrease

following treatment with MG (Fig. 7B). To verify more directly whether the ubiquitination of Hxt occurs following treatment with MG, we conducted a pull-down experiment with protein A-tagged Hxt2 and IgG beads followed by Western blotting using anti-ubiquitin antibodies. As shown in Fig. 7C, the proportion of Hxt2 having been ubiquitinated was increased following treatment with MG. Taken together, MG induces ubiquitination of Hxts in an Rsp5-dependent manner, and subsequently, endocytosis is induced to degrade them in the vacuole, which leads to a slow and gradual reduction of glucose uptake in the presence of MG.

#### *Phospholipase C negatively regulates endocytosis of Hxts*

Rsp5 contains the C2 domain which binds to phospholipids, such as phosphatidylinositols. The C2 domain of Rsp5 was verified to bind some species of phosphatidylinositols *in vitro* (37). Rsp5 has strong affinity for phosphatidylinositol 4,5-bisphosphate (PtdIns(4,5)P<sub>2</sub>), which is distributed in the plasma membrane in yeast cells. Since Hxts are located on the plasma membrane, Rsp5 needs to approach the plasma membrane to interact with its substrates, or Hxts. It may be conceivable that Rsp5 associates with the plasma membrane through PtdIns(4,5)P<sub>2</sub>. *PLC1* codes for the sole phospholipase C in *S. cerevisiae*. Since Plc1 hydrolyzes PtdIns(4,5)P<sub>2</sub> (23), it has an ability to bind PtdIns(4,5)P<sub>2</sub>. To explore the correlation between Rsp5 and Plc1, we investigated the effect of a Plc1-deficiency on the MG-induced endocytosis of Hxts. Intriguingly, strong fluorescence derived from Hxt1/2/3-GFPs was observed in vacuoles in *plc1Δ* cells despite an absence of MG (Fig. 8A). We investigated whether the fluorescence in the vacuoles is due to an increase in the expression of *HXTs*, thereby inducing the mislocalization of Hxts in vacuoles in *plc1Δ* cells. We monitored the expression of *HXT1~3* using *lacZ* fusion genes, but found no distinct differences (data not shown). Next, we constructed a *plc1Δrsp5<sup>wimp</sup>* mutant to monitor the localization of Hxt1/2/3-GFPs. As shown in Fig. 8B, GFP-tagged Hxt1~3 are essentially located on the plasma membrane in such a mutant. Therefore, it seems that the deletion of *PLC1* causes endocytosis of Hxt1~3 constitutively in an Rsp5-dependent manner. However, Hxt1/2/3-GFPs on the plasma

membrane disappeared following treatment with MG (Fig. 8A). These results indicate that the MG-induced endocytosis occurs independently of phospholipase C, although Plc1 can be defined as a negative regulator for endocytosis of Hxts under normal conditions.

#### *Involvement of TORC2 and Pkc1 in the MG-induced endocytosis of Hxt*

TORC2 (target of rapamycin complex 2) is a TOR kinase complex, consisting of Avo1, Avo2, Avo3, Bit61, and Lst8 (for review, see 38). It has been reported that TORC2 is involved in the endocytosis of Ste2, a G protein-coupled  $\alpha$ -factor receptor (39). To explore the involvement of TORC2 in the MG-induced endocytosis of Hxt, we used an RL25-1C strain whose *AVO1* expression is regulated by *GALI* promoter (40). Avo1 is an essential component of TORC2 (40). The integrity of TORC2 was maintained when RL25-1C cells were grown in galactose medium, but the unimpaired state was lost after the shift to glucose medium due to the reduced expression of *AVO1*. As shown in Fig. 9A, endocytosis of Hxt1-GFP did not occur when RL25-1C cells were treated with MG in glucose medium. These results suggest that TORC2 is involved in the MG-induced endocytosis of Hxt.

In this study, we have demonstrated that MG-induced endocytosis was repressed in the presence of Lat-B, a drug depolymerizing F actin. TORC2 plays crucial roles in the organization of the actin cytoskeleton (40). Besides TORC2, protein kinase C (Pkc1) is also involved in the organization of the actin cytoskeleton (41). We determined whether Pkc1 is also involved in the MG-induced endocytosis. Though *PKC1* is an essential gene, a *pkc1Δ* mutant is able to grow when sorbitol at high concentrations is supplemented in the medium (41). As shown in Fig. 9B, the MG-induced endocytosis occurred in the presence of sorbitol in wild-type cells. Intriguingly, the timing of the internalization of Hxt1/2/3-GFPs was delayed in *pkc1Δ* cells following treatment with MG. Pkc1 activates the downstream mitogen-activated protein (MAP) kinase cascade consisting of Bck1, Mkk1/Mkk2, and Mpk1, which is also thought to be involved in actin organization (41). However, the MG-induced endocytosis of Hxt1 occurred in *mpk1Δ* cells with essentially the same timing as that in wild-type cells (Fig. 9C). These results suggest that Pkc1, but not Mpk1 MAP kinase, is involved in the endocytosis of Hxts

in the presence of MG.

## DISCUSSION

### *Inhibition of Hxts by MG*

To gain a clue as to the correlation between MG and glucose homeostasis, we determined the effect of MG on glucose uptake using a yeast system. We found that MG inhibits the glucose-uptake activity of a yeast hexose transporter (Hxt) and a mammalian glucose transporter (GLUT). It is believed that glucose transporters have two glucose-binding sites, one facing the outside of the cell (import site) and the other the inside (export site), and conformational change occurs when glucose binds to either the import site or export site to pass through the transporter (19). Several drugs that inhibit mammalian glucose transporters have been found, many of which are thought to compete with glucose for the glucose-binding sites. For example, cytochalasin B binds to Trp<sup>388</sup> and Trp<sup>412</sup>, both of which are located within the estimated export site of human GLUT1, which leads to the inhibition of glucose uptake (19). By contrast, phloretin, phlorizin, and 4,6-*O*-ethylidene-D-glucose bind to the estimated import site of GLUT1 (42, 43). Cytochalasin B, phloretin, and phlorizin inhibit the activity of GLUT4 also (44). However, these drugs do not inhibit yeast Hxts (T. Kasahara and M. Kasahara, personal communications). Furthermore, as far as we know, no drugs capable of inhibiting yeast Hxts have been found. In that sense, our finding is the first to show a chemical that inhibits yeast Hxts.

It is known that MG reacts with Lys and Arg residues of proteins to form irreversible adducts, and with Cys residues reversibly (45). To gain a clue as to the mechanism how MG inhibits Hxt activity, we examined whether inhibition is reversible or not. Cells were treated with MG for 30 min, the timing at which Hxt activity was inhibited by approximately 60%, but a large proportion of Hxts has not yet been endocytosed, and subsequently cells were washed to remove MG and transferred to the fresh medium without MG. As shown in Fig. 1C, the levels of glucose uptake were reverted. These results suggest that the inhibitory effect of MG on Hxt activity is reversible. In contrast to mammalian GLUTs, no glucose-binding site has yet been identified in yeast Hxts, so we cannot assign which amino acid residues are the target of MG for inhibition; however,

Cys might be one of the candidate amino acid residues to be involved in the MG-dependent inhibition of Hxt. MG may be a useful tool for analyzing the function of Hxts.

We have demonstrated that MG inhibits the activity of not only yeast Hxts but also mammalian GLUT1 and GLUT4. Since MG is an endogenous metabolite, it exists in cells and plasma in mammals, *i. e.* it can be present both inside and outside of cells. Therefore, MG is accessible to the import site and export site of GLUT. Although the mechanism by which MG inhibits the activity of GLUTs has not yet been identified, our finding that exogenously added MG rapidly inhibits GLUT activity may provide new insights into the glucose homeostasis, which may be linked to diabetes mellitus. One of the pathologies of this disease is sustained hyperglycemia. As MG concentrations in plasma of diabetic patients are higher than those in healthy individuals (11-13), MG may inhibit GLUT1 constitutively expressed on the plasma membrane of many tissues, thereby lowering the efficacy of glucose uptake, which exacerbates the hyperglycemia. In addition, we have shown that MG inhibits GLUT4 also. Mammalian GLUT4 is usually contained in vesicles in cells carrying the insulin receptor. Upon the receipt of insulin, these GLUT4-containing vesicles are translocated to the plasma membrane, and subsequently, GLUT4 is exposed to the cell surface to take up glucose from blood (4). The fact that MG inhibits the activity of GLUT4 implies that MG interferes with insulin-responsive glucose uptake. Hence, the findings of this study using a yeast system lead us to propose that MG is involved in the onset and/or exacerbation of diabetes mellitus through impairment of glucose uptake.

### *Endocytosis of Hxts by MG*

We have demonstrated that Hxt1~3 are ubiquitinated and internalized following treatment with MG, then transported into vacuoles *via* the MVB pathway for degradation. It has been reported that phosphorylation is preceded by ubiquitination in the endocytosis of many plasma membrane-integral proteins. For example, Ste2 is phosphorylated by casein kinase homologues (Yck1 and Yck2) upon the receipt of  $\alpha$ -factor (46). Meanwhile, Hog1 phosphorylates Fps1, an aquaglyceroporin involved in the efflux of glycerol and uptake of acetic acid, thereby facilitating its degradation (47). We have previously reported that MG activates Hog1

MAP kinase (48), so we investigated whether the MG-induced endocytosis of Hxt1/2/3-GFPs is influenced in *hog1Δ* cells, but found no distinct differences in endocytosis between wild-type and *hog1Δ* cells (data not shown).

We revealed that Rsp5 plays a crucial role in the MG-induced endocytosis of Hxts. Rsp5 contains a WW domain, through which it is able to interact with the target protein to be ubiquitinated containing the PY motif (Leu/Pro-Pro-Xaa-Tyr) (35). Rsp5 functions as the E3 enzyme (ubiquitin ligase) for many transporters and permeases on the plasma membrane, however, it is rare for such cargo proteins to contain a canonical PY motif (35). So, Rsp5 needs to interact with an adaptor protein containing the PY motif that is able to physically interact with cargo proteins. Since Hxts do not contain a PY motif, an adaptor protein or arrestin-related trafficking adaptor (Art) is necessary for Rsp5 to physically interact with Hxts for ubiquitination. Indeed, Art4/Rod1 is involved in the endocytosis of Hxt6 (22). Generally, arrestins are able to bind to the phosphorylated cargo proteins on the plasma membrane (49, 50). Therefore, it is feasible that Hxts are phosphorylated following treatment with MG prior to endocytosis. Hxt7 lacking the cytoplasmic domain at the N terminus was hardly internalized and degraded under conditions where the endocytosis of Hxt7 was induced (high-glucose conditions) (51). It has been reported that the PEST (Pro-Glu-Ser-Thr) sequence found at the N terminus of Hxt7 is involved in the degradation (52, 53). On the other hand, the PES (Pro-Glu-Ser) sequence found in Hxts and maltose permeases has been also implicated in the degradation process (54). Both PEST and PES motives contain serine and/or threonine that have the potential to be phosphorylated. So, we tried to detect the phosphorylation of Hxt upon MG stress using protein A-tagged Hxt2 (Hxt2-PA) by pull-down experiments with IgG beads followed by Western blotting using anti-phospho-Ser and anti-phospho-Thr antibodies. However, as far as we could determine, phosphorylation of Hxt2 was not detected (data not shown). Nonetheless, we found that the timing of the MG-induced endocytosis of Hxt1/2/3-GFPs was delayed in *pkc1Δ* cells (Fig. 9B), so Pkc1 might be a candidate for the protein kinase responsible for the phosphorylation of Hxts for triggering endocytosis.

The endocytosis of Hxts was virtually dependent upon Rsp5. Strikingly, we found

that deficiency in Plc1 or Pkc1 affected the endocytosis of Hxts, therefore, both Plc1 and Pkc1 may influence the activity of Rsp5. The constitutive internalization of Hxt1~3 from the plasma membrane in *plc1Δ* cells was suppressed when the expression of Rsp5 was reduced (Fig. 8B), therefore, Plc1 might repress the function of Rsp5. One possible speculation is that Rsp5 and Plc1 might compete with each other for the binding to PtdIns(4,5) $P_2$  on the plasma membrane. Rsp5 contains C2 domain, which has the affinity to PtdIns(4,5) $P_2$ , enriched in the plasma membrane. Recently, Kaminska *et al.* (55) reported that GFP-tagged Rsp5 was located on the plasma membrane. Meanwhile, Plc1 has the PH (pleckstrin homology) domain (56), through which it binds to PtdIns(4,5) $P_2$ . Therefore, if Plc1 is deleted, Rsp5 may be able to access PtdIns(4,5) $P_2$  more easily, which allows Rsp5 to interact with cargo proteins thereby inducing the constitutive endocytosis of Hxts.

By contrast, since MG-induced endocytosis was delayed in *pkc1Δ* cells, Pkc1 may be involved in the activation of Rsp5 following treatment with MG. Recently, a cationic amino acids transporter (CTA-1) in HEK293 cells was ubiquitinated by activation of protein kinase C (PKC), which is carried out by Nedd4-1 and Nedd4-2, mammalian orthologues of Rsp5 (57). Therefore, it is conceivable that Pkc1 may activate Rsp5 in yeast cells.

In contrast to Pkc1, Mpk1 MAP kinase, which lies downstream of Pkc1, was not likely to be involved in the MG-induced endocytosis of Hxts (Fig. 9C). Regarding a role of Mpk1 in the endocytosis of Hxts, Soulard *et al.* (58) have reported that Mpk1 is involved in the rapamycin-induced endocytosis of Hxt1. Rapamycin is a specific inhibitor of TORC1 (target of rapamycin complex 1) (40). We also verified that rapamycin induces endocytosis of Hxt1~3 in an Rsp5-dependent manner using Hxt1/2/3-GFPs (Supplemental Fig. S1). Soulard *et al.* (58) reported that inhibition of TORC1 with rapamycin induces the phosphorylation of Bcy1 at Thr<sup>129</sup>, by which Bcy1 is activated as a negative regulatory subunit of protein kinase A (PKA). Schmelzle *et al.* (59) have reported that the rapamycin-induced endocytosis of Hxt1 was suppressed under conditions where the Ras/cAMP pathway was activated, *i. e.* deletion of *BCY1*, or introduction of the constitutively activated allele of *RAS2* (Ras2<sup>Val19</sup>). These results imply that PKA

negatively regulates endocytosis of Hxt1. Meanwhile, Souldard *et al.* (58) reported that Sch9, a direct substrate of TORC1, inactivates Mpk1. In addition, they reported that Mpk1 phosphorylates Thr<sup>129</sup> of Bcy1 directly in the presence of rapamycin, which leads to deactivation of PKA (58). Collectively, rapamycin treatment deactivates Sch9, which inactivates PKA through the Mpk1-mediated phosphorylation of Bcy1 at Thr<sup>129</sup>, thereby inducing endocytosis. If MG provokes the same regulatory circuit as rapamycin does, the Mpk1-mediated phosphorylation of Bcy1 might occur, leading to the inhibition of PKA thereby inducing endocytosis of Hxts. However, we have demonstrated that the MG-induced endocytosis of Hxts occurred even in *mpk1Δ* cells (Fig. 9C). Furthermore, we found that the MG-induced endocytosis of Hxts

occurred in *sch9Δ* cells (Fig. 9D). Taken together, MG and rapamycin seem to induce endocytosis of Hxts *via* different pathways. Although Pkc1 lies upstream of the Mpk1 MAP kinase cascade, Pkc1 seems to provoke the endocytosis of Hxts in the presence of MG through a pathway in which Mpk1 is not involved.

Yeast has been used to study many pivotal biological events, because basic mechanistic principals are similar between yeasts and higher eukaryotes. This would also be the case for glucose uptake. The analysis of the intracellular distribution of GLUT1 and GLUT4 in mammalian cells following treatment with MG on the basis of our findings regarding the distribution of yeast Hxts would provide further insight into the correlation between MG and glucose homeostasis as well as diabetes mellitus.

## REFERENCES

1. Lagunas, R. (1993) *FEMS Microbiol. Rev.* **10**, 229–242
2. Walmsley, A. R., Barrett, M. P., Bringaud, F., and Gould, G. W. (1988) *Trends Biochem. Sci.* **23**, 476-481
3. Pao, S. S., Paulsen, I. T., and Saier, M. H. Jr. (1998) *Microbiol. Mol. Biol. Rev.* **62**, 1-34
4. Huang, S., and Czech, M. P. (2007) *Cell Metab.* **5**, 237-252
5. Dyer, D. G., Blackledge, J. A., Katz, B. M., Hull, C. J., Adkisson, H. D., Thorpe, S. R., Lyons, T. J., and Baynes, J. W. (1991) *Z. Ernährungswiss* **30**, 29-45
6. Inoue, Y., and Kimura, A. (1995) *Adv. Microb. Physiol.* **37**, 177-227
7. Inoue, Y., Maeta, K., and Nomura, W. (2011) *Semin. Cell. Dev. Biol.* **22**, 278-284
8. Kalapos, M. P. (1999) *Toxicol. Lett.* **110**, 145-175
9. Turk, Z. (2010) *Physiol. Res.* **59**, 147-156
10. McLellan, A. C., Thornalley, P. J., Benn, J., and Sonksen, P. H. (1994) *Clin. Sci. (Lond.)* **87**, 21-29
11. Beisswenger, P. J., Howell, S. K., Touchette, A. D., Lal, S., and Szwegold, B. S. (1999) *Diabetes* **48**, 198-202
12. Beisswenger, P. J., Howell, S. K., O'Dell, R. M., Wood, M. E., Touchette, A. D., and Szwegold, B. S. (2001) *Diabetes Care* **24**, 726-732
13. Lapolla, A., Flamini, R., Dalla Vedova, A., Senesi, A., Reitano, R., Fedele, D., Basso, E., Seraglia, R., and Traldi, P. (2003) *Clin. Chem. Lab. Med.* **41**, 1166-1173
14. Yki-Järvinen, H., Helve, E., and Koivisto, V. A. (1987) *Diabetes* **36**, 892-896
15. Thurmond, D. C., and Pessin, J. E. (2001) *Mol. Membr. Biol.* **18**, 237-245
16. Mueckler, M. (1994) *Eur. J. Biochem.* **219**, 713-725
17. Thorens, B. (1996) *Am. J. Physiol.* **270**, G541-553
18. Rea, S., and James, D. E. (1997) *Diabetes* **46**, 1667-1677
19. Uldry, M., and Thorens, B. (2004) *Pflugers. Arch.* **447**, 480-489
20. Mueckler, M., Caruso, C., Baldwin, S. A., Panico, M., Blench, I., Morris, H. R., Allard, W. J., Lienhard, G. E., and Lodish, H. F. (1985) *Science* **229**, 941-945
21. Özcan, S., and Johnston, M. (1999) *Microbiol. Mol. Biol. Rev.* **63**, 554-569
22. Nikko, E., and Pelham, H. R. (2009) *Traffic* **10**, 1856-1867
23. Flick, J. S., and Thorner, J. (1993) *Mol. Cell. Biol.* **13**, 5861-5876
24. Izawa, S., Takemura, R., and Inoue, Y. (2004) *J. Biol. Chem.* **279**, 35469-35478

25. Roosen, J., Engelen, K., Marchal, K., Mathys, J., Griffioen, G., Cameroni, E., Thevelein, J. M., De Virgilio, C., De Moor, B., and Winderickx, J. (2005) *Mol. Microbiol.* **55**, 862-880
26. Kruckeberg, A. L., Ye, L., Berden, J. A., and van Dam, K. (1999) *Biochem. J.* **339**, 299-307
27. Bagnat, M., and Simons, K. (2002) *Proc. Natl. Acad. Sci. U.S.A.* **99**, 14183-14188
28. Wiczorke, R., Dlugai, S., Krampe, S., and Boles, E. (2003) *Cell Physiol. Biochem.* **13**, 123-134
29. Ghaemmaghami, S., Huh, W. K., Bower, K., Howson, R. W., Belle, A., Dephoure, N., O'Shea, E. K., and Weissman, J. S. (2003) *Nature* **425**, 737-741
30. Katzmann, D. J., Odorizzi, G., and Emr, S. D. (2002) *Nat. Rev. Mol. Cell Biol.* **3**, 893-905
31. Nikko, E., and André, B. (2007) *Traffic* **8**, 566-581
32. Kranz, A., Kinner, A., and Kölling, R. (2001) *Mol. Biol. Cell* **12**, 711-723
33. Harrison, J. C., Bardes, E. S., Ohya, Y., and Lew, D. J. (2001) *Nat. Cell Biol.* **3**, 417-420
34. Engqvist-Goldstein, A. E., and Drubin, D. G. (2003) *Annu. Rev. Cell. Dev. Biol.* **19**, 287-332
35. Léon, S., and Haguenaer-Tsapis, R. (2009) *Exp. Cell Res.* **315**, 1574-1583
36. Rotin, D., Staub, O., and Haguenaer-Tsapis, R. (2000) *J. Membr. Biol.* **176**, 1-17
37. Dunn, R., Klos, D. A., Adler, A. S., and Hicke, L. (2004) *J. Cell Biol.* **165**, 135-144
38. Powers, T., Aronova, S., and Niles, B. (2010) *The Enzymes* **27**, 177-197
39. deHart, A. K., Schnell, J. D., Allen, D. A., Tsai, J. Y., and Hicke, L. (2003) *Mol. Biol. Cell* **14**, 4676-4684
40. Loewith, R., Jacinto, E., Wullschleger, S., Lorberg, A., Crespo, J. L., Bonenfant, D., Oppliger, W., Jenoe, P., and Hall, M. N. (2002) *Mol. Cell* **10**, 457-468
41. Levin, D. E. (2005) *Microbiol. Mol. Biol. Rev.* **69**, 262-291
42. Kasahara, T., and Kasahara, M. (1996) *Biochem. J.* **315**, 177-182
43. Mueckler, M., Weng, W., and Kruse, M. (1994) *J. Biol. Chem.* **269**, 20533-20538
44. Kasahara, T., and Kasahara, M. (1997) *Biochim. Biophys. Acta* **1324**, 111-119
45. Maeta, K., Izawa, S., Okazaki, S., Kuge, S., and Inoue, Y. (2004) *Mol. Cell. Biol.* **24**, 8753-8764
46. Hicke, L., Zanolari, B., and Riezman, H. (1998) *J. Cell Biol.* **141**, 349-358
47. Mollapour, M., and Piper, P. W. (2007) *Mol. Cell. Biol.* **27**, 6446-6456
48. Maeta, K., Izawa, S., and Inoue, Y. (2005) *J. Biol. Chem.* **280**, 253-260
49. Ferguson, S. S., Downey, W. E. 3rd, Colapietro, A. M., Barak, L. S., Ménard, L., and Caron, M. G. (1996) *Science* **271**, 363-366
50. Lohse, M. J., Benovic, J. L., Codina, J., Caron, M. G., and Lefkowitz, R. J. (1990) *Science* **248**, 1547-1550
51. Krampe, S., and Boles, E. (2002) *FEBS Lett.* **513**, 193-196
52. Hein, C., Springael, J. Y., Volland, C., Haguenaer-Tsapis, R., and André, B. (1995) *Mol. Microbiol.* **18**, 77-87
53. Marchal, C., Haguenaer-Tsapis, R., and Urban-Grimal, D. (1998) *Mol. Cell. Biol.* **18**, 314-321
54. Brondijk, T. H., van der Rest, M. E., Plum, D., de Vries, Y., Stingl, K., Poolman, B., and Konings, W. N. (1998) *J. Biol. Chem.* **273**, 15352-15357
55. Kaminska, J., Spiess, M., Stawiecka-Mirota, M., Monkaityte, R., Haguenaer-Tsapis, R., Urban-Grimal, D., Winsor, B., and Zoladek, T. (2011) *Eur. J. Cell. Biol.* **90**, 1016-1028
56. Rebecchi, M. J., and Pentylala, S. N. (2000) *Physiol. Rev.* **80**, 1291-1335
57. Vina-Vilaseca, A., Bender-Sigel, J., Sorkina, T., Closs, E. I., and Sorkin, A. (2011) *J. Biol. Chem.* **286**, 8697-8706
58. Soulard, A., Cremonesi, A., Moes, S., Schütz, F., Jenö, P., and Hall, M. N. (2010) *Mol. Biol. Cell* **21**, 3475-3486
59. Schmelzle, T., Beck, T., Martin, D. E., and Hall, M. N. (2004) *Mol. Cell. Biol.* **24**, 338-351
60. Levin, D. E., and Bartlett-Heubusch, E. (1992) *J. Cell Biol.* **116**, 1221-1229
61. Balguerie, A., Bagnat, M., Bonneu, M., Aigle, M., and Breton, A. M. (2002) *Eukaryot.*

### Acknowledgment

We thank Dr. T. Kasahara (Teikyo University, Japan) for valuable discussions, and generous gift of plasmids (Hxt1mnx-pVT, Hxt2mnx-pVT, pVT102-U/His-Xa-human-GLUT1, and pVT102-U/rat-GLUT4) and antibodies (anti-Hxt1, anti-Hxt2, anti-GLUT1, and anti-GLUT4 antibodies), Dr. E. Boles (Heinrich-Heine-Universität, Germany) for EBY.S7 and EBY.F4-1, Dr. K. van Dam (The University of Amsterdam, The Netherlands) for KY73, Dr. M. N. Hall (University of Basel, Switzerland) for TB50a and RL25-1C, Dr. A. Breton (CNRS, France) for the Pma1-GFP and Rvs161-GFP plasmids, Dr. D. E. Levin (Boston University, USA) for DL100 and DL376, and Dr. H. R. Pelham (MRC Laboratory of Molecular Biology, UK) for EN44.

Abbreviations used are: MFS, major facilitator superfamily; AGE, advanced glycation end product, MG, methylglyoxal; Hxt, hexose transporter; Lat-B, latrunculin B; WCE, whole cell extract; MVB, multivesicular body; PtdIns(4,5) $P_2$ , phosphatidylinositol 4,5-bisphosphate; TORC2, target of rapamycin complex 2; MAP, mitogen-activated protein; TORC1, target of rapamycin complex 1; PKA, protein kinase A.

### FOOTNOTE

This study was partially supported by a Grant-in-Aid for Scientific Research from the Ministry of Education, Science, Sports and Culture of Japan, and Grants from Institution of Fermentation, Osaka, Japan to Y.I.

### Figure Legends

**Fig. 1.** Effect of MG on glucose uptake. *A*, cells (YPH250) were cultured in SD medium until a log phase of growth, and MG at various concentrations was added. After 15 min, glucose uptake was determined as described in Materials and Methods. *B*, cells (YPH250) were treated with 10 mM MG for the period indicated, and glucose uptake was determined. *C*, glucose uptake was measured after addition of 10 mM MG periodically. After 30 min, cells were collected by centrifugation, washed and suspended in fresh SD medium without MG, and glucose uptake was determined (0 min was relatively taken as 100%). Data are averages for three independent experiments  $\pm$  standard deviations.

**Fig. 2.** MG induces internalization and degradation of Hxts. *A*, cells (YPH250) carrying Hxt1-GFP, Hxt2-GFP, or Hxt3-GFP were cultured in SD medium until a log phase of growth, and treated with 10 mM MG for the period indicated. The distribution of each GFP-tagged Hxt was observed using a fluorescence microscope. DIC, differential interference contrast. *B*, cells carrying Pma1-GFP or Rvs161-GFP were treated with 10 mM MG for the period indicated, and the distribution of each GFP-tagged protein was determined. *C*, cells carrying Hxt1-GFP, Hxt2-GFP, or Hxt3-GFP were treated with MG as described in *A*, membrane and soluble fractions were prepared, and the amount of each GFP protein was determined by Western blotting.

**Fig. 3.** Doa4 is involved in the endocytosis of Hxts. Wild type and *doa4* $\Delta$  mutant (BY4741 background) carrying Hxt1-GFP, Hxt2-GFP, or Hxt3-GFP were cultured in SD medium until a

log phase of growth, and treated with 10 mM MG for the period indicated. The distribution of each Hxt-GFP was observed using a fluorescence microscope. Vacuolar membrane was stained by FM4-64.

**Fig. 4.** MG inhibits the activity of Hxts. *A*, cells (YPH250) carrying Hxt1-GFP, Hxt2-GFP, or Hxt3-GFP were cultured in SD medium until a log phase of growth, and treated with 100  $\mu$ M latrunculin B (Lat-B) for 20 min prior to treatment with 10 mM MG. The distribution of each Hxt-GFP was observed using a fluorescence microscope. *B*, cells were cultured in SD medium until a log phase of growth, and 100  $\mu$ M Lat-B was added. After 20 min, [ $^{14}$ C]-glucose was added. Glucose uptake in the first 5 min and 60 min after addition of MG was determined as described in Materials and Methods. Data are averages for three independent experiments  $\pm$  standard deviations.

**Fig. 5.** MG inhibits Hxt activity. *A*, K73 (*hxt1-7 $\Delta$* ) cells carrying Hxt1mnx-pYT harboring *HXT1* (encoding a low-affinity glucose transporter) or Hxt2mnx-pVT harboring *HXT2* (encoding a high-affinity glucose transporter) were cultured in SD medium. A membrane fraction was prepared from each transformant as described in Materials and Methods. Expression of *HXT1* and *HXT2* was verified by Western blotting using anti-Hxt1 and anti-Hxt2 antibodies, respectively.  $\alpha$ -Pma1 indicates the loading control for the membrane fraction. *B*, glucose uptake of each transformant was determined as described in Materials and Methods. Data are averages for three independent experiments  $\pm$  standard deviations.

**Fig. 6.** MG inhibits mammalian GLUTs. *A*, EBY.S7 (*hxt $\Delta$* ) cells carrying human GLUT1 cDNA were cultured in SD medium until a log phase of growth, and a membrane fraction was prepared as described in Materials and Methods. Expression of GLUT1 cDNA was verified by Western blotting using anti-GLUT1 antibodies. Glucose uptake in the first 5 min in the presence of Lat-B was determined. *B*, EBY.F4-1 (*hxt $\Delta$* ) cells carrying rat GLUT4 cDNA were cultured in SD medium until a log phase of growth, and the expression of GLUT4 and glucose uptake were determined as described in *A*.  $\alpha$ -Pma1 indicates the loading control for the membrane fraction.

**Fig. 7.** Hxt is ubiquitinated in an Rsp5-dependent manner. *A*, cells (YPH250 background) of the wild type (WT) and *rsp5<sup>wimp</sup>* carrying Hxt1-GFP, Hxt2-GFP, or Hxt3-GFP were cultured in SD medium until a log phase of growth, and treated with 10 mM MG for the period indicated. The distribution of each GFP-tagged Hxt was observed using a fluorescence microscope. *B*, *rsp5<sup>wimp</sup>* cells (YPH250 background) carrying Hxt1-GFP, Hxt2-GFP, or Hxt3-GFP were treated with MG as described in *A*, soluble and membrane fractions were prepared, and the amount of each GFP protein or Pma1 was determined by Western blotting. The intensity of each Hxt-GFP band in membrane fractions was quantified by densitometry, and normalized with Pma1 as a loading control of each lane. The level of each Hxt-GFP protein at 0 min was relatively taken as 1.0. Data are averages for three independent experiments  $\pm$  standard deviations. *C*, MBY242 cells carrying protein A-tagged Hxt2 (*HXT2-PA*) were cultured in SD medium until a log phase of growth and treated with MG for the period indicated in the figure. A membrane fraction was prepared by ultracentrifugation. This was followed by a pull-down experiment using IgG beads. Ubiquitination ( $\alpha$ -Ub) and the amount of Hxt2-PA ( $\alpha$ -PA) were determined using anti-ubiquitin and anti-PA antibodies, respectively, as described in Materials and Methods.

**Fig. 8.** Hxts are constitutively internalized in *plc1 $\Delta$*  cells. *A*, *plc1 $\Delta$*  cells (YPH250 background) carrying Hxt1-GFP, Hxt2-GFP, or Hxt3-GFP were cultured in SD medium until a log phase of growth, and treated with 10 mM MG for 120 min. The distribution of each GFP-tagged protein was observed using a fluorescence microscope. *B*, cells (YPH250 background) of the wild type (WT), *plc1 $\Delta$* , *rsp5<sup>wimp</sup>*, and *plc1 $\Delta$ rsp5<sup>wimp</sup>* carrying Hxt1-GFP, Hxt2-GFP, or Hxt3-GFP were cultured in SD medium until a log phase of growth, and the distribution of each GFP-tagged Hxt was determined.

**Fig. 9.** Involvement of TORC2 and Pkc1 in the MG-induced endocytosis of Hxts. *A*, TB50a (wild type, WT) and RL25-1C (TB50a background with *GAL1* promoter-driven *AVO1*, *pGAL-AVO1*) cells carrying Hxt1-GFP were cultured in SGal medium until a log phase of growth, and transferred to SD medium. After 10 h, 10 mM MG was added, and the distribution of Hxt1-GFP was determined using a fluorescence microscope. *B*, cells (DL100 background) of the wild type (WT) and *pkc1* $\Delta$  carrying Hxt1-GFP were cultured in SD medium containing 0.5 M sorbitol, and 10 mM MG was added. The distribution of Hxt1/2/3-GFPs was determined using a fluorescence microscope. *C*, cells (DL100 background) of the wild type (WT) and *mpk1* $\Delta$  carrying Hxt1-GFP were cultured in SD medium containing 0.5 M sorbitol until a log phase of growth, and the distribution of Hxt1-GFP was determined after addition of 10 mM MG. *D*, cells (YPH250 background) of the wild type (WT) and *sch9* $\Delta$  carrying Hxt1-GFP, Hxt2-GFP or Hxt3-GFP were treated with 10 mM MG for the period indicated.

Table 1

## Yeast strains used in this study

Strain	Relevant genotype/description	Source/reference
YPH250	<i>MATa trpΔ1-1 his3-Δ200 leu2-Δ1 lys2-801 ade2-101 ura3-52</i>	Lab stock
BY4741	<i>MATa his3Δ1 leu2Δ0 met15Δ0 ura3Δ0</i>	Invitrogen
<i>rsp5<sup>wimp</sup></i>	YPH250, <i>natMX</i> was inserted into the promoter of <i>RSP5</i>	This study
<i>plc1Δ</i>	YPH250, <i>plc1Δ::HIS3</i>	This study
<i>plc1Δrsp5<sup>wimp</sup></i>	YPH250, <i>plc1Δ::HIS3 rsp5<sup>wimp</sup></i>	This study
<i>sch9Δ</i>	YPH250, <i>sch9Δ::TRP1</i>	This study
<i>doa4Δ</i>	BY4741, <i>doa4Δ::KanMX4</i>	This study
<i>mpk1Δ</i>	DL100, <i>mpk1Δ::KanMX4</i>	This study
EN44	BY4741, <i>natMX</i> was inserted into the promoter of <i>RSP5</i>	22
MBY242	<i>MATa his4 ura3 leu2 lys2 bar1 HXT2-PA::URA3</i>	27
YJF32	<i>MATa ura3-52 lys2-801 amber ade2-101 ochre trp1-Δ63 his3-Δ200 leu2-Δ1 plc1Δ::HIS3</i>	23
TVH301	<i>MATa ade2-1 can1-100 his3-11,15 leu2-3,112 trp1-1 ura3-1 sch9::TRP1</i>	25
KY73	<i>MATa hxt1Δ::HIS3::Δhxt4 hxt5::LEU2 hxt2Δ::HIS3 hxt3Δ::LEU2::hxt6 hxt7::HIS3 gal2Δ::DR ura3-52 his3-11,15 leu2-3,112 MAL2 SUC2 GAL MEL</i>	26
EBY.S7	<i>MATa hxt1-17Δ gal2Δ agt1Δ stl1Δ leu2-3,112 ura3-52 trp1-289 his3-Δ1 MAL2-8c SUC2 hxtΔ fgy1-1</i>	28
EBY.F4-1	<i>MATa hxt1-17Δ gal2Δ agt1Δ stl1Δ leu2-3,112 ura3-52 trp1-289 his3-Δ1 MAL2-8c SUC2 hxtΔ fgy1-1 fgy41</i>	28
TB50a	<i>MATa his3 leu2-3, 112 ura3-52 rme1 trp1</i>	40
RL25-1C	TB50a, [ <i>KanMX4</i> ]- <i>GAL1p-3HA-AVO1</i>	40
DL100	<i>MATa leu2-3,112 trp1-1 ura3-52 his4 can1</i>	60
DL376	DL100, <i>pkc1Δ::LEU2</i>	60

Table 2

## Plasmids used in this study

Plasmid	Description	Source/reference
pHXT1-GFP	pRS306 (integrate-type, <i>URA3</i> marker) backbone, for replacement of endogenous <i>HXT1</i> with <i>HXT1-GFP</i>	This study
pHXT2-GFP	pRS306 (integrate-type, <i>URA3</i> marker) backbone, for replacement of endogenous <i>HXT2</i> with <i>HXT2-GFP</i>	This study
pHXT3-GFP	pRS306 (integrate-type, <i>URA3</i> marker) backbone, for replacement of endogenous <i>HXT3</i> with <i>HXT3-GFP</i>	This study
pRS316+PMA1-GFP	pRS316 ( <i>CEN</i> -type, <i>URA3</i> marker) harboring Pma1-GFP	61
pFL44+RVS161-GFP	pFL44 ( <i>CEN</i> -type, <i>URA3</i> marker) harboring Rvs161-GFP	61
YIp358R+HXT1-lacZ	YIp358R (integrate-type, <i>URA3</i> marker) backbone, for fusion with <i>HXT1</i> and <i>lacZ</i>	This study
YIp358R+HXT2-lacZ	YIp358R (integrate-type, <i>URA3</i> marker) backbone, for fusion with <i>HXT2</i> and <i>lacZ</i>	This study
YIp358R+HXT3-lacZ	YIp358R (integrate-type, <i>URA3</i> marker) backbone, for fusion with <i>HXT3</i> and <i>lacZ</i>	This study
Hxt1mnx-pVT	pVT102-U (2 $\mu$ -type, <i>URA3</i> marker) backbone, for expression of <i>HXT1</i>	62
Hxt2mnx-pVT	pVT102-U (2 $\mu$ -type, <i>URA3</i> marker) backbone, for expression of <i>HXT2</i>	62
pVT102-U/His-Xa-human-GLUT1	pVT102-U (2 $\mu$ -type, <i>URA3</i> marker) backbone, for expression of human <i>GLUT1</i> cDNA	Kasahara, T. unpublished
pVT102-U/rat-GLUT4	pVT102-U (2 $\mu$ -type, <i>URA3</i> marker) backbone, for expression of rat <i>GLUT4</i> cDNA	Kasahara, T. unpublished

Figure 1 Yoshida et al.

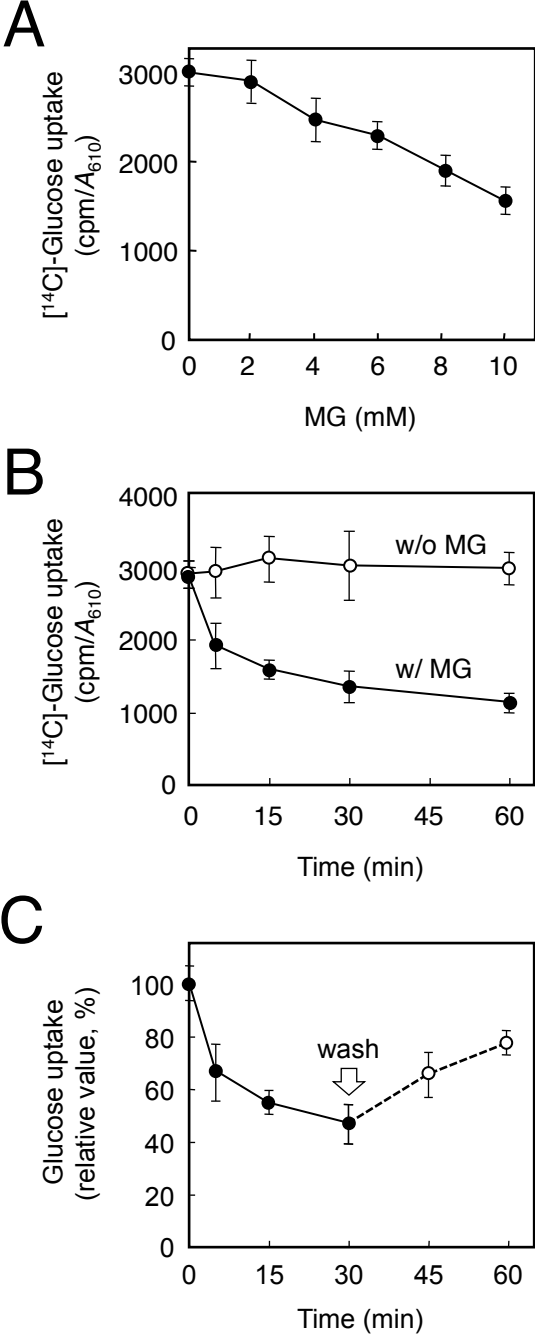


Figure 2 Yoshida et al.

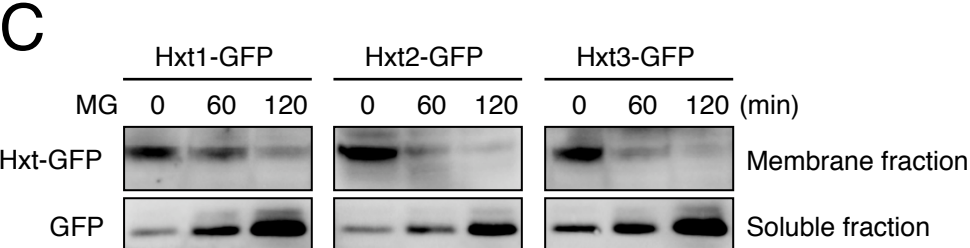
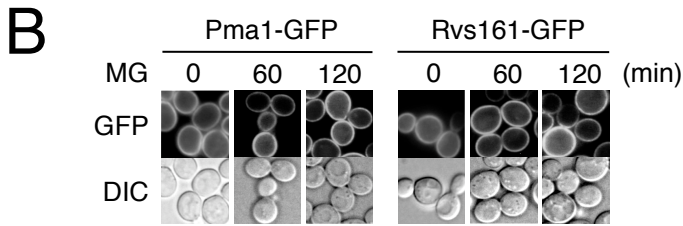
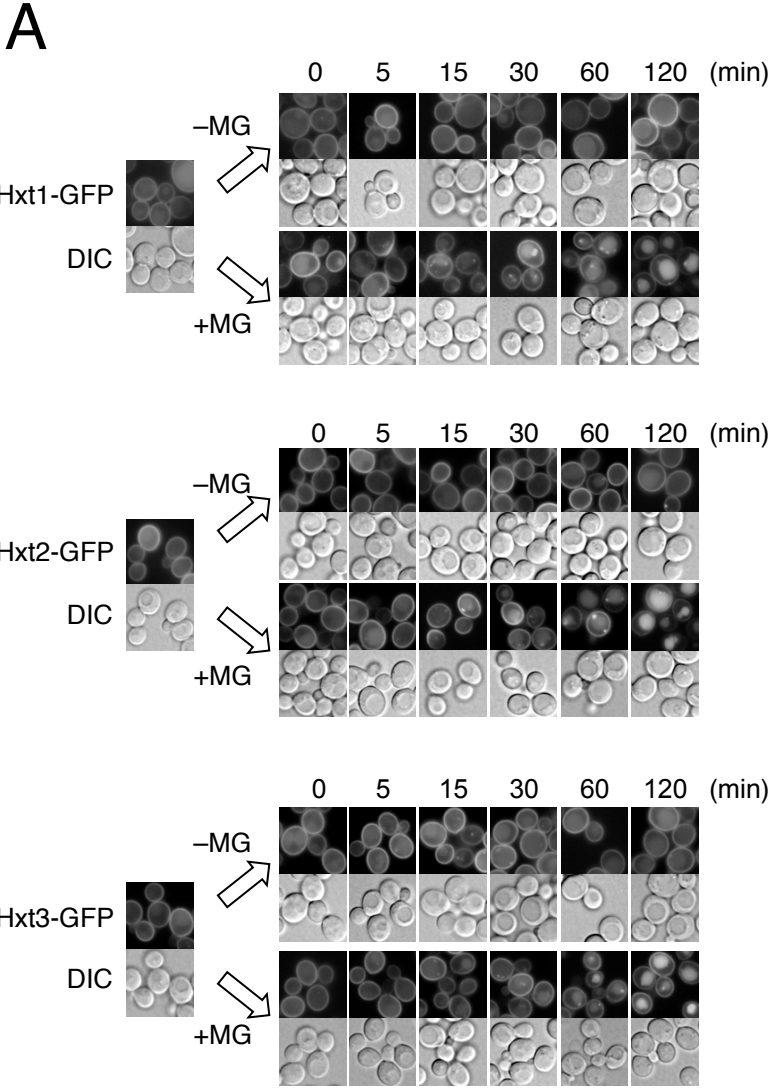


Figure 3 Yoshida et al.

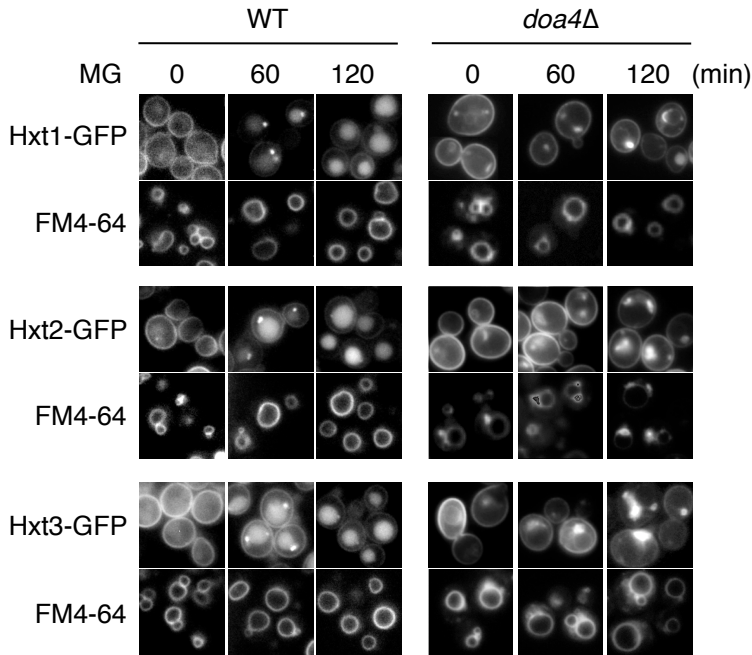


Figure 4 Yoshida et al.

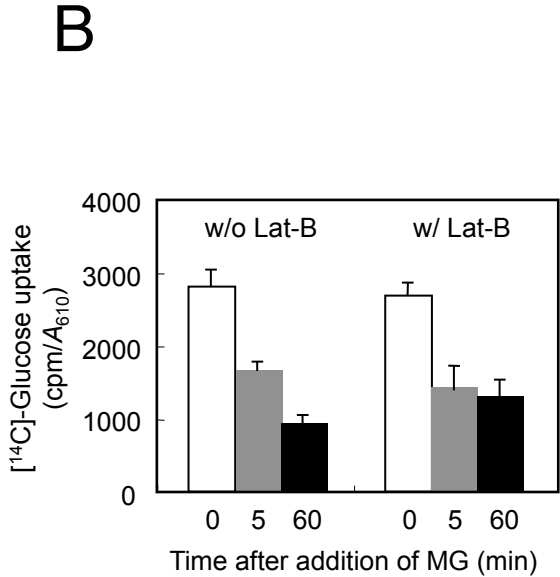
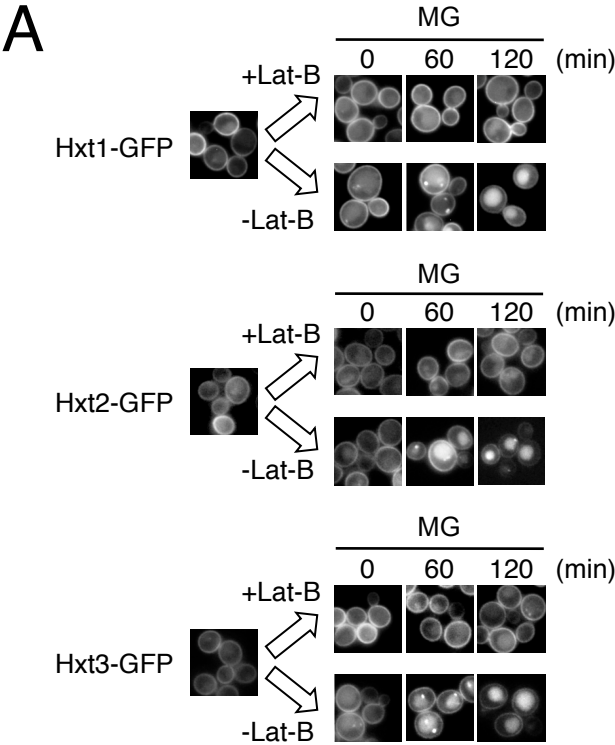


Figure 5 Yoshida et al.

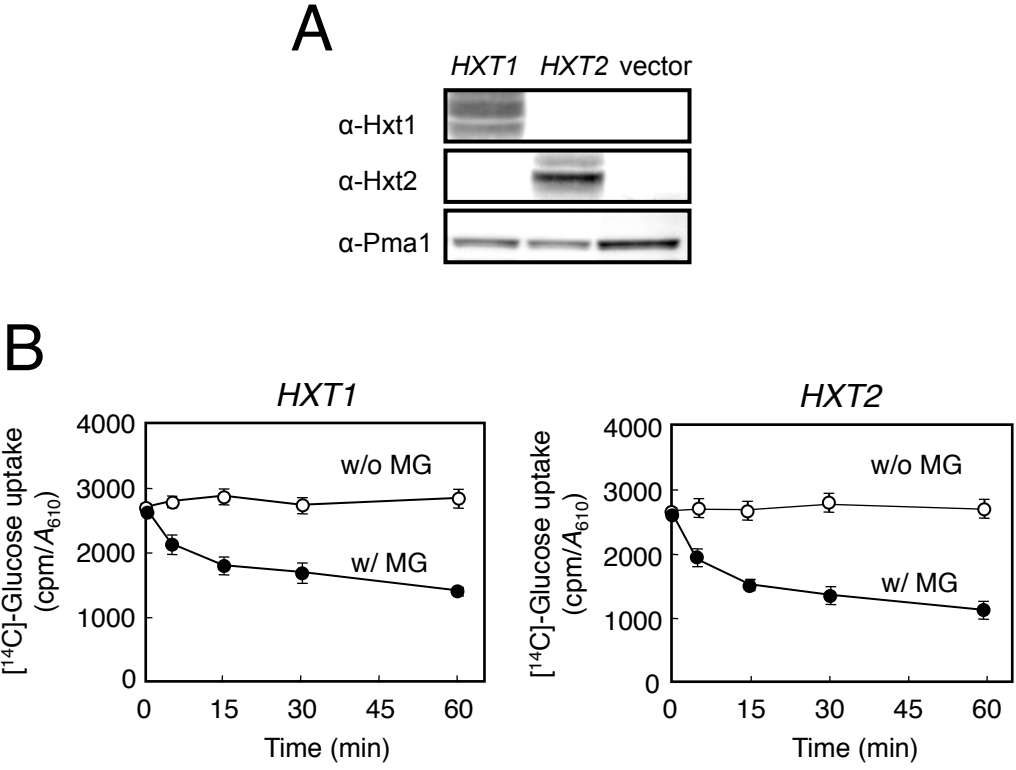


Figure 6 Yoshida et al.

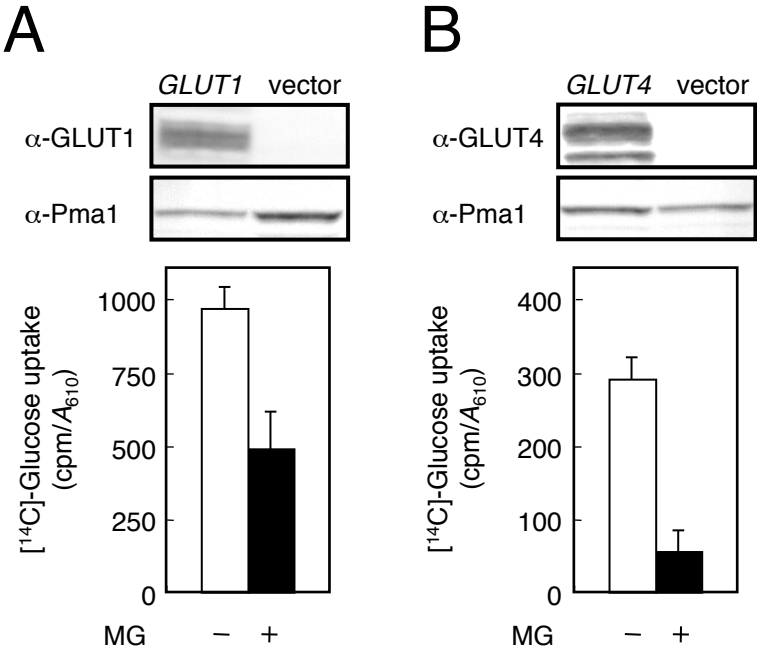


Figure 7 Yoshida et al.

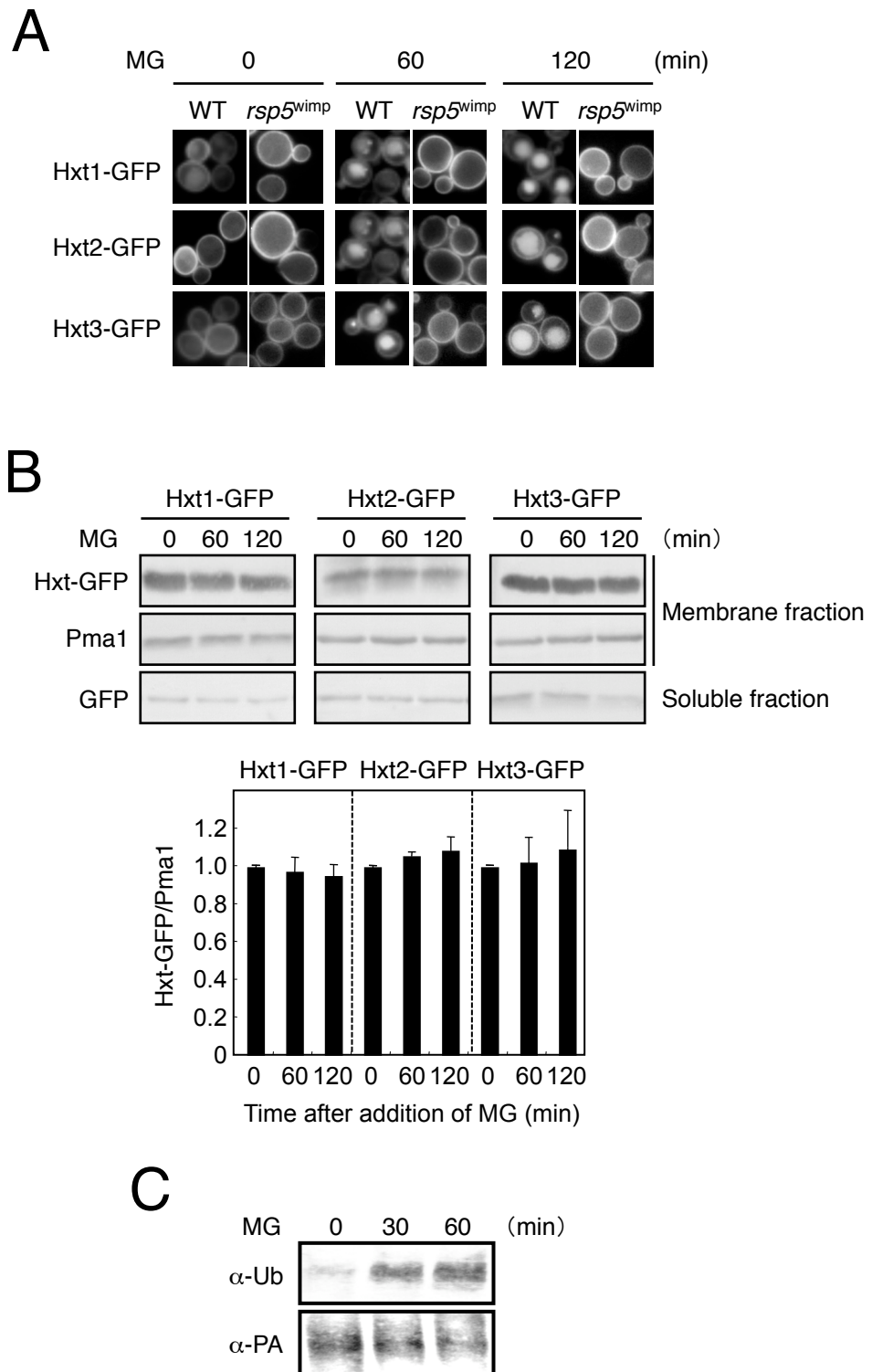


Figure 8 Yoshida et al.

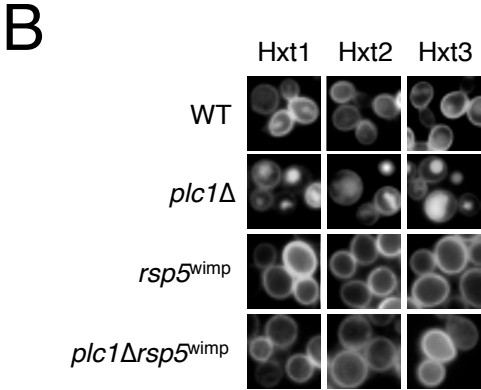
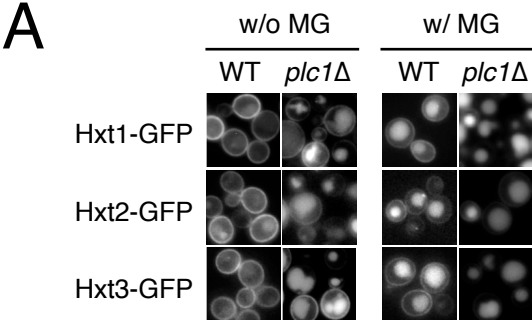
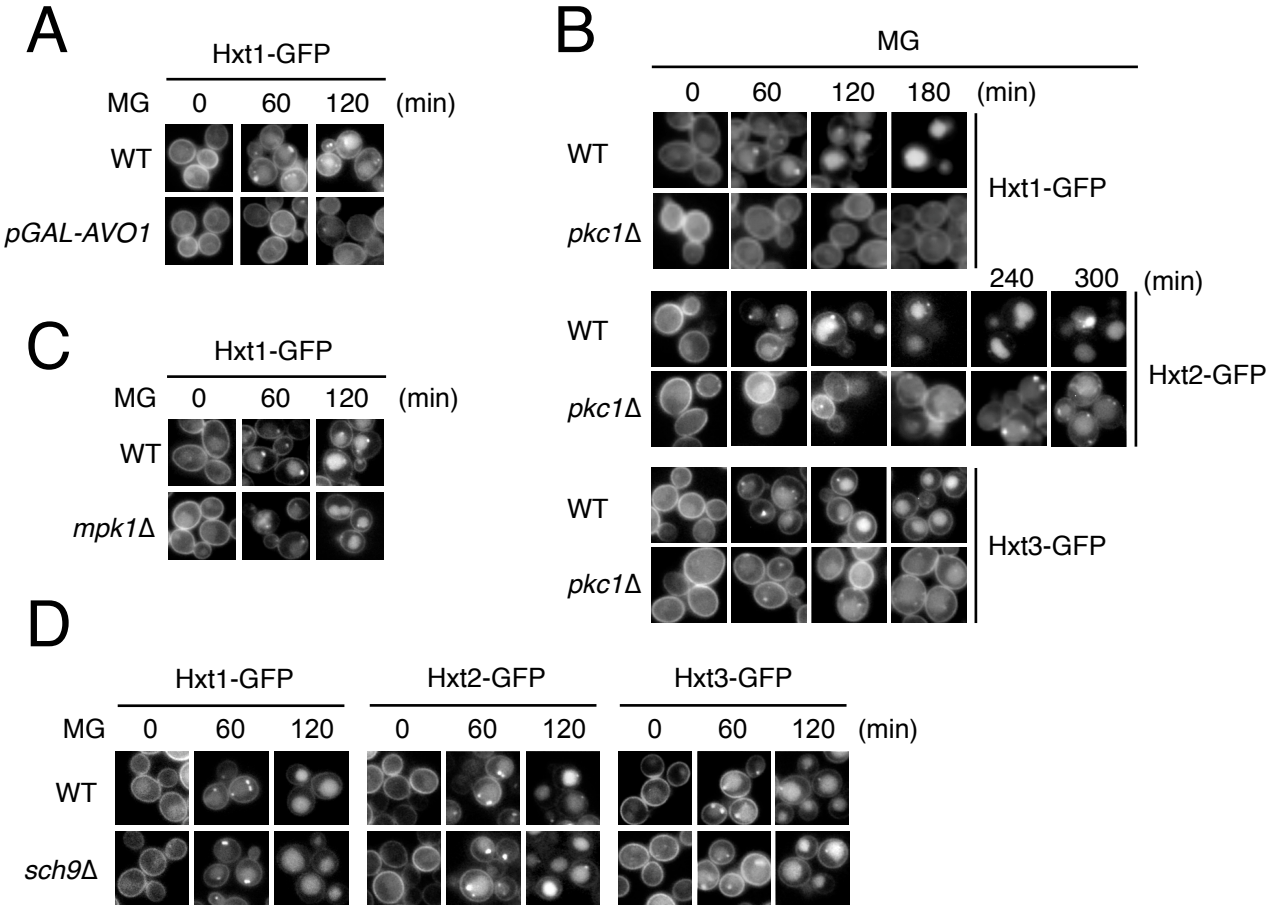


Figure 9 Yoshida et al.



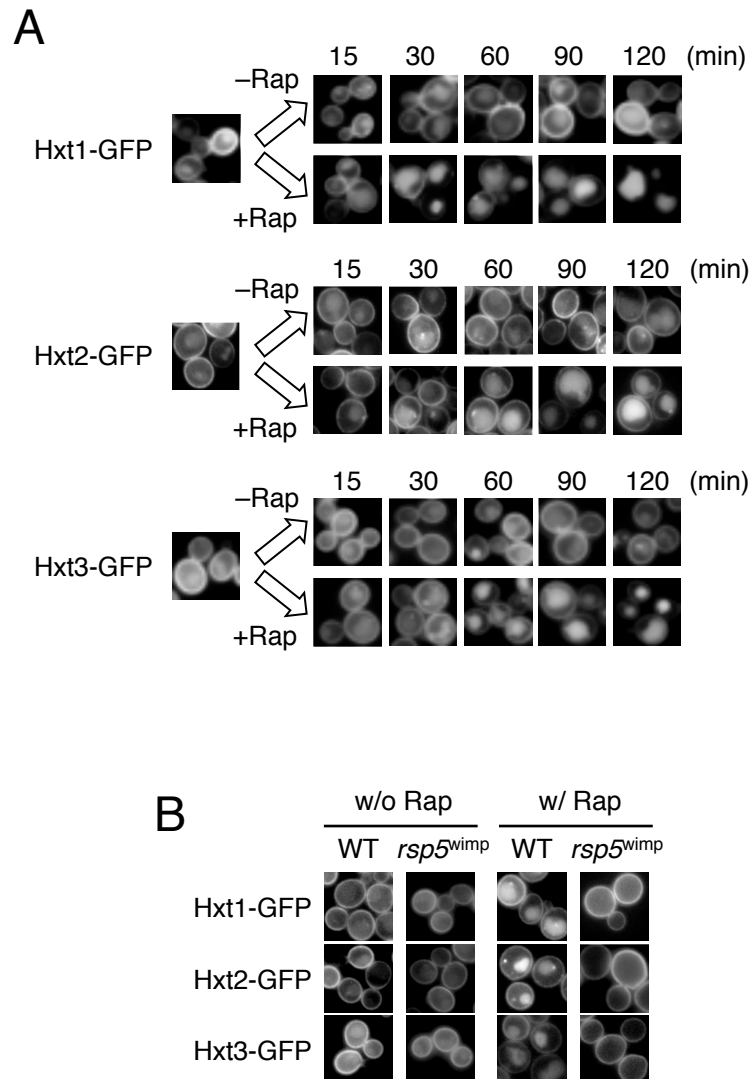
Supplemental Table S1

Primers used in this study

Primer	Sequence
RSP5-F	5'-GACCAAATTGCAGTGATCTTCATGGTG-3'
RSP5-R-2	5'-TCGCTGCGGATGTAGATTTGGTTTGGTAAC-3'
PLC1-F	5'-CCTATATACAAGGATAAAGTGGTGAAAGTC-3'
PLC1-R-2	5'-TTTGATGGTGATATCATCTTTCAGTGTCTC-3'
SCH9-F	5'-TGCTCAGCTCATCCATTTGCTGGT-3'
SCH9-R	5'-TCACAGCGAAGCGTTTACTTAAGCC-3'
HXT1-F-XbaI	5'-CCAATCTAGATGATATGTATGGTCGTAGAA-3'
HXT1-F-XhoI	5'-GTTCTCGAGATTTCCCTGCTAAACAAACTCT-3'
HXT2-F-XbaI	5'-TCGGACGCTCTAGACTGGTTTGATCGTTGGT-3'
HXT2-F-XhoI	5'-TATAACTCGAGATTCCTCGGAAACTCTTTTTTCTTT-3'
HXT3-F-XbaI	5'-TGTGCAATCTAGAGTTCCATTAGGTTTGTG-3'
HXT3-F-XhoI	5'-AGCGTCTCGAGATTTCTTGCCGAACATTTTCTTGTA-3'
Hxt1-GFP-F-SacI	5'-GTTGAGCTCAGACTAACCATCATAACTTCC-3'
Hxt2-GFP-F-SacI	5'-TTTGAGCTCCACGTGGCTTTGCTTTCCCCG-3'
Hxt3-GFP-F-SacI	5'-TTCGAGCTCGTTTGCATCTTCTTGCATTTG-3'
HXT1-lacZ F	5'-TACCTCTAAAGAGTGTGACCAACTGA-3'
HXT1-lacZ R	5'-ATCGGGAGGAATTCATGATTTTACGTAT-3'
HXT2-lacZ F	5'-TTCTAGTCGACAGGTCAGTTAAGGCACAGA-3'
HXT2-lacZ R	5'-AGTAGGAATTCCAGACATTATGTTGCTTTA-3'
HXT3-lacZ F	5'-TCTCTCCGGCGTCGACTTTCAACCTAAGG-3'
HXT3-lacZ R	5'-TGGAGGAATTCATGATTGTTTAACTCAG-3'

Underlines indicate the sites of restriction enzymes designed. Details are described in the text.

Supplemental Fig. S1



**Supplemental Fig. S1.** MG induces internalization and degradation of Hxts. *A*, cells (YPH250) carrying Hxt1-GFP, Hxt2-GFP, or Hxt3-GFP were cultured in SD medium until a log phase of growth, and treated with 200 ng/ml rapamycin (Rap) for the period indicated. The distribution of each GFP-tagged Hxt was observed using a fluorescence microscope. *B*, *rsp5<sup>wimp</sup>* cells (YPH250 background) carrying Hxt1-GFP, Hxt2-GFP, or Hxt3-GFP were treated with 200 ng/ml rapamycin (Rap) for 60 min.